

Prospects for Detecting Gravitational Waves from Eccentric Subsolar Mass Compact Binaries

YI-FAN WANG (王一帆)^{1,2} AND ALEXANDER H. NITZ^{1,2}

¹*Max-Planck-Institut für Gravitationsphysik (Albert-Einstein-Institut), D-30167 Hannover, Germany*

²*Leibniz Universität Hannover, D-30167 Hannover, Germany*

ABSTRACT

Due to their small mass, subsolar mass black hole binaries would have to be primordial in origin instead of the result of stellar evolution. Soon after formation in the early universe, primordial black holes can form binaries after decoupling from the cosmic expansion. Alternatively, primordial black holes as dark matter could also form binaries in the late universe due to dynamical encounters and gravitational-wave braking. A significant feature for this channel is the possibility that some sources retain nonzero eccentricity in the LIGO/Virgo band. Assuming all dark matter is primordial black holes with a delta function mass distribution, $1M_{\odot} - 1M_{\odot}$ binaries formed in this late-universe channel can be detected by Advanced LIGO and Virgo with their design sensitivities at a rate of $\mathcal{O}(1)$ /year, where 12%(3%) of events have eccentricity at a gravitational-wave frequency of 10 Hz, $e^{10\text{Hz}} \geq 0.01(0.1)$, and nondetection can constrain the binary formation rate within this model. Third generation detectors would be expected to detect subsolar mass eccentric binaries as light as $0.01M_{\odot}$ within this channel, if they accounted for the majority of the dark matter. Furthermore, we use simulated gravitational-wave data to study the ability to search for eccentric gravitational-wave signals using a quasi-circular waveform template bank with Advanced LIGO design sensitivity. For a match-filtering targeted search, assuming binaries with a delta function mass of $0.1(1)M_{\odot}$ and the eccentricity distribution derived from this late-universe formation channel, 41%(6%) of the signals would be missed compared to the ideal detection rate due to the mismatch in the gravitational-wave signal from eccentricity.

Keywords: Gravitational Waves — Eccentricity — Primordial Black Holes

1. INTRODUCTION

Gravitational-wave astronomy has gradually evolved into a routine method for observing compact binaries comprising black holes and/or neutron stars. Up to now, over 50 gravitational-wave events have been identified by Advanced LIGO (Aasi et al. 2015) and Virgo (Acerese et al. 2015), all from compact binary coalescences (Nitz et al. 2019; Abbott et al. 2020). These detections have had significant astrophysical implications, including inferring stellar population properties (The LIGO Scientific Collaboration et al. 2020a), testing the validity of general relativity (The LIGO Scientific Collaboration et al. 2020b), and determining the value of the Hubble constant (Abbott et al. 2017).

In addition to routine detection, gravitational-wave data analysis is also searching for exotic hypothesized

objects, such as primordial black holes (Abbott et al. 2018a, 2019; Nitz & Wang 2021). Primordial black holes are hypothesized to form by direct collapse in dense regions of the early universe (Zel'dovich & Novikov 1967; Hawking 1971; Carr & Hawking 1974) and are consistent with the properties required for a candidate of cold dark matter (Carr & Kuhnel 2020). A variety of astrophysical observations including gravitational lensing have searched for primordial black holes and placed upper limits on the abundance with their null results, which shows that primordial black holes with a single mass are not likely to account for all dark matter (see, e.g., Carr & Kuhnel (2020) and Green & Kavanagh (2021) for recent reviews). Nevertheless, as gravitational-wave astronomy provides new opportunities to observe stellar-mass black holes, we investigate the event rate and prospects for searching for gravitational waves emitted from binary primordial black holes in the LIGO/Virgo sensitive band ($\sim 10 - 1000$ Hz). In particular, we focus on subsolar mass binary mergers with nonzero eccentricity.

There are two viable ways for primordial black holes to form binaries. In the early universe, after their initial formation, a nearby pair of primordial black holes can form a binary if the gravitational attraction is strong enough to decouple them from the cosmic expansion (Nakamura et al. 1997; Sasaki et al. 2016; Boehm et al. 2021). To be detected by gravitational-wave detectors, the binaries would have had sufficient time to circularize their orbits, thus the gravitational-wave signals are not expected to have eccentricity by the time they enter the LIGO and Virgo sensitive band. On the other hand, primordial black hole binaries may also form by dynamical capture due to gravitational-wave braking in the late-universe in dark matter halos. A significant feature for this formation channel is the retention of nonzero eccentricity in the LIGO/Virgo band if the binaries form at close separation. This latter scenario is the focus of this work.

Bird et al. (2016) has studied the event rate of GW150914-like, i.e., a $30M_\odot$ binary black hole merger. Their results show that the event rate is consistent with the empirical rate estimated from GW150914 (Abbott et al. 2016a,b). However, it is challenging to confirm that GW150914 is indeed primordial in origin and not the result of stellar evolution, leaving the question still open. Cholis et al. (2016) has investigated the eccentricity distribution for $30M_\odot$ binaries in the late-universe scenario. Meanwhile, given conventional stellar evolution models, subsolar mass ($\leq 1M_\odot$) compact binary coalescence can only be due to primordial black holes, instead of stellar products, because they are lighter than the minimum mass of neutron stars (Timmes et al. 1996; Suwa et al. 2018). Therefore, in this work we only consider the mass range $[0.01, 1] M_\odot$, which is a smoking gun for primordial black holes, extending the work of Bird et al. (2016) and Cholis et al. (2016) to subsolar mass region. Primordial black holes in this mass range are predicted by a variety of formation theories, e.g., early-universe Quantum Chromodynamics (QCD) phase transition (Jedamzik 1997; Byrnes et al. 2018; Carr et al. 2021).

In Section 2, assuming a delta function distribution of mass, we first estimate the event rate and eccentricity distribution of subsolar mass primordial black hole binaries formed in dark matter halos. The merger rate of subsolar mass binaries is shown to be higher than that of $30M_\odot$ binary primordial black holes as considered in Bird et al. (2016) by one to two orders of magnitude. With design sensitivity, the Advanced LIGO and Virgo observatories would be expected to detect one $1M_\odot - 1M_\odot$ binary with eccentricity $e^{10\text{Hz}} \geq 0.1$ at a gravitational-wave frequency of 10 Hz with ~ 10 years

of observation, if the fraction of the primordial black hole in dark matter is 100%. Third generation detectors would detect primordial black hole binaries with a single mass varying from $0.01M_\odot$ to $1M_\odot$ and eccentricity distribution derived from this late-universe formation channel. Nondetection in the future would put constraints on the event rate modeling. In Section 3, we investigate the capability of the current match-filtering search pipeline using a quasi-circular waveform template bank to identify signals with eccentricity by simulated gravitational-wave data. Results show that 41% and 6% of the signals would be missed compared to the idealized maximum for $0.1M_\odot - 0.1M_\odot$ and $1M_\odot - 1M_\odot$ binaries, respectively, arising from the mismatch of gravitational-wave signals from eccentricity. Section 4 presents the discussions and conclusions.

2. EVENT RATE AND ECCENTRICITY DISTRIBUTION

In this section we consider the event rate and eccentricity distribution of compact binaries formed in the late universe through two-body encounters for a delta function mass distribution which we allow to vary within $[0.01, 1]M_\odot$. More complex mechanisms may also induce eccentric binaries, such as three-body interaction via Kozai-Lidov effects (Kozai 1962; Lidov 1962), but they are not considered in this work and investigations will be left for the future.

We briefly review the two-body dynamics for primordial black hole binary formation following Maggiore (2008); Peters & Mathews (1963); Turner (1977); O’Leary et al. (2009); Bird et al. (2016); Cholis et al. (2016). Specifically, we derive the overall event rate for primordial black hole binary coalescence with a component mass $M_{\text{PBH}} = 0.01/0.1/1 M_\odot$. To aid in comparison to other works in this field, we state our eccentricity distributions at a fiducial dominant-mode gravitational-wave frequency of 10 Hz, which is denoted by $e^{10\text{Hz}}$.

Two black holes can form a binary in an encounter due to gravitational-wave emission. The binary formation criterion is that the released gravitational-wave energy δE_{GW} exceeds the two-body kinetic energy

$$\delta E_{\text{GW}} \geq \frac{1}{2}\mu v_{\text{rel}}^2, \quad (1)$$

where $\mu = m_1 m_2 / (m_1 + m_2)$ is the reduced mass, m_1 and m_2 are the component masses of the binary, and v_{rel} is the relative velocity of two black holes. In this work we only consider equal-mass primordial black hole binaries, therefore we set $m_1 = m_2 = M_{\text{PBH}}$.

At a Newtonian order, the released gravitational-wave energy is (Peters & Mathews 1963; Turner 1977)

$$\delta E_{\text{GW}} = \frac{8}{15} \frac{G^{7/2}}{c^5} \frac{(m_1 + m_2)^{1/2} m_1^2 m_2^2}{r_p^{7/2}} f(e) \quad (2)$$

where G is the Newton gravitational constant, c is the speed of light, r_p is the closest distance at encounter, which is the pericenter distance for an elliptical orbit, and $f(e)$ is a function of eccentricity e . By inserting $f(e) = 425\pi/(32\sqrt{2})$ when $e = 1$ into Eqs. (1) and (2), one obtains the cross section for binary formation

$$\sigma = 2\pi \left(\frac{85\pi}{6\sqrt{2}} \right)^{2/7} \frac{G^2 (m_1 + m_2)^{10/7} (m_1 m_2)^{2/7}}{c^{10/7} v_{\text{rel}}^{18/7}} \quad (3)$$

where $\sigma = \pi b_{\text{max}}^2$ by definition, and b_{max} is the maximum impact parameter. Meanwhile, the impact parameter b is related to r_p by

$$r_p = \frac{b^2 v_{\text{rel}}^2}{2G(m_1 + m_2)} \quad (4)$$

when $G(m_1 + m_2) \gg b v_{\text{rel}}^2$, which is satisfied in this study.

Since we aim to investigate the scenario where primordial black holes are dark matter, we assume the number density of primordial black holes follows that of dark matter. Specifically, for a dark matter halo with virial mass M_{vir} , we use the Navarro-Frenk-White (NFW) density profile (Navarro et al. 1996) to model the mass density

$$\rho_{\text{NFW}}(r) = \frac{\rho_c}{\frac{r}{r_c} \left(1 + \frac{r}{r_c} \right)^2}, \quad (5)$$

where r is the radial distance to the halo center, and ρ_c and r_c are the characteristic mass density and characteristic radius of the NFW profile, respectively.

The binary primordial black hole formation rate is given by Bird et al. (2016) as

$$\mathcal{R}(M_{\text{vir}}) = 4\pi \int_0^{R_{\text{vir}}} \frac{r^2}{2} \left(\frac{f_{\text{PBH}} \rho_{\text{NFW}}(r)}{M_{\text{PBH}}} \right)^2 \langle \sigma v_{\text{rel}} \rangle dr, \quad (6)$$

where R_{vir} is the halo virial radius, f_{PBH} is the mass fraction of primordial black holes in dark matter, and the angle bracket is averaged with respect to the relative velocity distribution, which is modeled to be Maxwell-Boltzmann distribution

$$P(v_{\text{rel}}) = N_0 \left[\exp \left(-\frac{v_{\text{rel}}^2}{v_{\text{max}}^2} \right) - \exp \left(-\frac{v_{\text{vir}}^2}{v_{\text{max}}^2} \right) \right] \quad (7)$$

in which v_{vir} is the circular velocity at virial radius, v_{max} is the maximum circular velocity, and N_0 is the normalization factor. As demonstrated by Bird et al. (2016),

the merger happens shortly after the formation of a binary, therefore the formation rate (Eq. (6)) is identical to the event rate for coalescence of binary primordial black holes. Eq. (6) can be integrated analytically, the result is

$$\mathcal{R}(M_{\text{vir}}) = \left(\frac{85\pi}{6\sqrt{2}} \right)^{2/7} \frac{2\pi G^2 f_{\text{PBH}}^2 M_{\text{vir}}^2 D(v_{\text{max}})}{3c r_s^3 g^2(C)} \times \left[1 - \frac{1}{(1+C)^3} \right], \quad (8)$$

where $C = R_{\text{vir}}/r_c$ is the concentration parameter for dark matter halo, $g(C) = \ln(1+C) - C/(1+C)$ and

$$D(v_{\text{rel}}) = \int_0^{v_{\text{vir}}} P(v_{\text{rel}}; v_{\text{max}}) \left(\frac{2v}{c} \right)^{3/7} dv. \quad (9)$$

Finally, the overall event rate for binary primordial black hole coalescence is obtained by taking the sum of the contributions from all dark matter halos

$$\mathcal{R}_{\text{PBH}} = \int \mathcal{R}(M_{\text{vir}}) \frac{dN}{dM_{\text{vir}}} dM_{\text{vir}} \quad (10)$$

We have made use of the python code `colossus` (Diemer 2018) to generate the dark matter halo mass function dN/dM_{vir} using the parameterized formula fitting to an N-body simulation proposed by Tinker et al. (2008), and the concentration-dark matter halo mass relation proposed by Prada et al. (2012). We have tested systematics by using Raeymaekers (2007) for N-body simulation fits for the dark matter halo mass function, and Dutton & Macciò (2014) for the concentration-halo mass relation. The results show a different choice of dark matter halo population modeling will not change the final event rate by orders of magnitude.

Assuming $f_{\text{PBH}} = 100\%$, the result of Eq. (10) is shown in Fig. 1. The main contribution to the integral in Eq. (10) is from low-mass dark matter halos, therefore the result depends sensitively on the lower end for halo mass. To illustrate the dependence on lower mass cutoff $M_{\text{vir}}^{\text{low}}$, we plot \mathcal{R}_{PBH} as a function of $M_{\text{vir}}^{\text{low}}$ in Fig. 1. Also note that the integrand of Eq. (10) does not depend on M_{PBH} due to compensation between the primordial black hole number density and the cross section. To determine the lower limit of the dark matter halo mass for $M_{\text{PBH}} = 0.01/0.1/1 M_{\odot}$, we follow the criterion by Eq. (11) of Bird et al. (2016) requiring that the dark matter halo evaporation time scale due to dynamical relaxation exceeds the dark energy domination time scale ($\sim 3 \times 10^9$ yr). This choice results in the lower integral limit of Eq. (10) being $0.3/3/21 M_{\odot}$ for $M_{\text{PBH}} = 0.01/0.1/1 M_{\odot}$. Choosing a lighter dark matter halo cutoff would contribute more binary primordial

black hole merger events if the halos would not have evaporated at present and the NFW profile is still preserved. High resolution dark matter N-body simulations are needed to precisely resolve the smallest structure of subsolar mass primordial black hole halos but this is beyond the scope of this paper.

With the above choices of lower integral cutoff, as shown in Fig. 1, the event rate for $M_{\text{PBH}} = 0.01/0.1/1M_{\odot}$ is 528/140/45 $\text{Gpc}^{-3} \text{yr}^{-1}$. As a comparison, for $M_{\text{PBH}} = 30M_{\odot}$, the event rate is $\mathcal{O}(1) \text{Gpc}^{-3} \text{yr}^{-1}$ as computed in Bird et al. (2016). Therefore, the merger rate of subsolar primordial black holes increases by one to two orders of magnitude compared to that of $30M_{\odot}$.

To compare with observations, the sensitive volume, which is defined to be the orientation-averaged volume assuming a match-filtering signal-to-noise ratio (S/N) > 8 (Abbott et al. 2018b), is $\mathcal{O}(10^{-7})/\mathcal{O}(10^{-4})/\mathcal{O}(10^{-2}) \text{Gpc}^3$ for $M_{\text{PBH}} = 0.01/0.1/1M_{\odot}$ for Advanced LIGO at its design sensitivity. Given the above estimated event rate, under our assumption of delta function mass distribution, the second generation detectors are capable of detecting $M_{\text{PBH}} = 1M_{\odot}$ sources with a $\mathcal{O}(1)$ year run, and would not be likely to observe $0.1M_{\odot}$ and $0.01M_{\odot}$ sources. Third generation detectors such as the Cosmic Explorer (Reitze et al. 2019) and Einstein Telescope (Punturo et al. 2010) are expected improve the sensitive volume by three orders of magnitude compared to the second generation, thus they would be able to detect a delta function mass of $M_{\text{PBH}} = 0.1M_{\odot}$ source every $\mathcal{O}(0.1) \text{yr}$, and a $0.01M_{\odot}$ source with a $\mathcal{O}(10) \text{yr}$ observation time. Conversely, a nondetection in the future would put constraints on the abundance of primordial black holes formed in this late-universe channel.

We also compare the binary coalescence rate to that derived from primordial black hole binary formation in the early universe. Using the derivation by Sasaki et al. (2016), the merger rate is $\mathcal{O}(10^8)/\mathcal{O}(10^7)/\mathcal{O}(10^6) \text{Gpc}^{-3} \text{yr}^{-1}$ for $M_{\text{PBH}} = 0.01/0.1/1 M_{\odot}$ assuming $f_{\text{PBH}} = 100\%$. Therefore, an early-universe formation scenario dominates the event rate for subsolar mass compact binary coalescence, but this formation channel is not expected to yield eccentric binaries because they would have been circularized in the local universe. There are also model uncertainties under active investigation about what fraction of primordial black hole binaries would be disrupted after formation in the early universe (Ali-Haïmoud et al. 2017; Raidal et al. 2019; Vaskonen & Veermäe 2020; Jedamzik 2021). If a significant fraction are disrupted, the merger rate for the early-universe formation channel would be suppressed. Recently, Boehm et al. (2021) also pointed out that the merger rate of

early Universe formation channel is overestimated by reanalysis of the primordial black hole binary formation criterion.

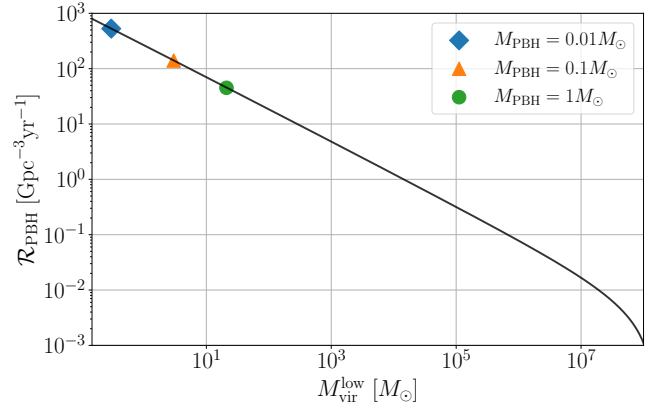


Figure 1. Event rate for binary primordial black hole merger as a function of the lower cutoff of dark matter halo mass. The markers are the event rate for $M_{\text{PBH}} = 0.01/0.1/1M_{\odot}$, which are 528/140/45 $\text{Gpc}^{-3} \text{yr}^{-1}$, respectively.

Compact binaries formed through dynamical interaction may retain eccentricity within the ground-based gravitational-wave detector frequency band. In the following we determine the eccentricity distribution for binary primordial black hole merger events following the references O’Leary et al. (2009); Cholis et al. (2016).

Right after formation, the initial semi-major distance of a binary is given by

$$a_0 = \frac{Gm_1m_2}{2|E_f|} \quad (11)$$

where $E_f = 1/2\mu v_{\text{rel}}^2 - \delta E_{\text{GW}}$. Combining Eqs. (4) and (11) and inserting the relation $r_{p,0} = a_0(1 - e_0)$, one obtains an expression for the initial eccentricity at binary formation of

$$e_0(m_1, m_2, v_{\text{rel}}, b) = \sqrt{1 - \frac{2|E_f|b^2v_{\text{rel}}^2}{(m_1 + m_2)m_1m_2}} \quad (12)$$

After formation of the binary, the semi-major distance a and the eccentricity e gradually decay due to gravitational-wave emission, the time evolution equation is given by (Peters 1964)

$$\begin{aligned} \frac{da}{dt} &= -\frac{64}{5} \frac{G^3 m_1 m_2 (m_1 + m_2)}{c^5 a^3 (1 - e^2)^{7/2}} \left(1 + \frac{73}{24} e^2 + \frac{37}{96} e^4 \right), \\ \frac{de}{dt} &= -\frac{304}{15} \frac{G^3 m_1 m_2 (m_1 + m_2) e}{c^5 a^4 (1 - e^2)^{5/2}} \left(1 + \frac{121}{304} e^2 \right). \end{aligned} \quad (13)$$

Combining Eq. (13) yields the expression for da/de which can be integrated analytically, the result is

$$a(e) = a_0 \frac{\kappa(e)}{\kappa(e_0)} \quad (14)$$

where $\kappa(e)$ is a function of e

$$\kappa(e) = \frac{e^{12/19}}{1 - e^2} \left(1 + \frac{121}{304} e^2 \right)^{870/2299}. \quad (15)$$

Substituting Eqs. (11) and (12) and $a = \sqrt[3]{G(m_1 + m_2)/\pi^2 f_{\text{GW}}^2}$ from the Kepler's third law where the frequency $f_{\text{GW}} = 10\text{Hz}$, the nonlinear Eq. (14) for $e^{10\text{Hz}}$ can be solved by numerically finding the root.

As $e^{10\text{Hz}}$ depends on e_0 , which in turn depends on the initial relative velocity v_{rel} and the impact parameter b for two black holes, we compute the relative velocity distribution by taking the derivative of \mathcal{R}_{PBH} with respect to v_{rel} . The results are presented in Fig. 2. It can be seen that the initial relative velocities for $M_{\text{PBH}} = 0.01/0.1/1 M_\odot$ peak at 5/10/25 m/s, respectively, which approximately correspond to the typical velocity of the lightest dark matter halo in the integral Eq. (10), because the merger events from the low-mass dark matter halo dominate the event rate.

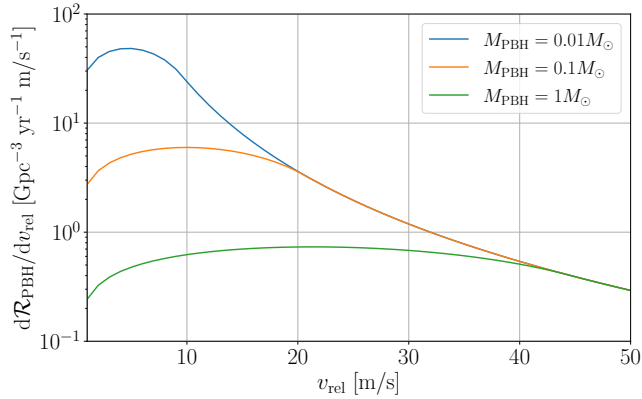


Figure 2. The binary primordial black hole event rate density with respect to the relative velocity v_{rel} at the formation of primordial black hole binaries for $M_{\text{PBH}} = 0.01/0.1/1 M_\odot$.

We use a Monte Carlo method to simulate a population of binary primordial black holes with masses $0.01/0.1/1 M_\odot$, respectively, each containing $\sim 10^6$ sources, to obtain the distribution of $e^{10\text{Hz}}$. The square of the impact parameter, b^2 , is chosen to be uniformly distributed in $[r_{\text{ISCO}}^2, b_{\text{max}}^2]$ (Cholis et al. 2016), where r_{ISCO} is the innermost stable circular orbit for a Schwarzschild black hole (6 times the Schwarzschild radius), b_{max} is given by Eq. (3). The initial relative velocity is drawn from the distribution in Fig. 2.

The results for the distribution of $e^{10\text{Hz}}$ are shown in Fig. 3 by the solid lines with the corresponding probability density distribution shown on the left vertical axis. To assist understanding, we also plot the cumulative probability distribution in Fig. 3 as shown by the solid lines converging to 100% at the right vertical axis. As seen from the figure, lighter primordial black holes tend to retain larger eccentricity. For $M_{\text{PBH}} = 0.01/0.1/1 M_\odot$, up to 89%/40%/12% of the total inspiral events have $e^{10\text{Hz}} \geq 0.01$, and up to 29%/9%/3% have $e^{10\text{Hz}} \geq 0.1$. To connect these estimates with observations, assuming $f_{\text{PBH}} = 100\%$, we find that second generation detectors would be expected to detect an eccentric binary coalescence with $M_{\text{PBH}} = 1 M_\odot$ within a few years observation time, while the third generations are expected to probe the eccentric events down to $0.01 M_\odot$ with 10^3 times of sensitive volume than Advanced LIGO and Virgo. In addition, third generation detectors are designed increase sensitivity at frequencies of $\sim 2 - 5$ Hz, where the eccentricity will be more significant. Third generation detectors show promise for detecting or constraining our understanding of eccentric binaries.

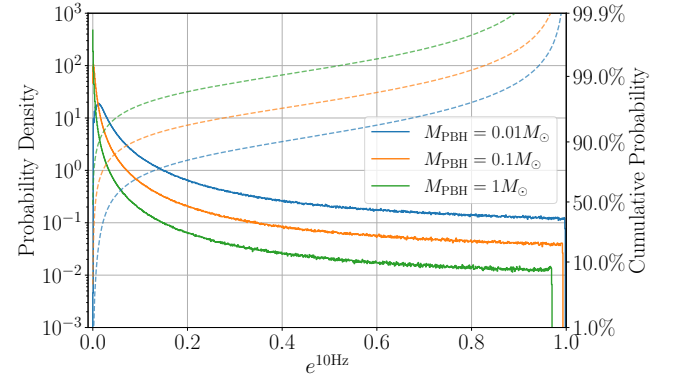


Figure 3. The probability density distribution (solid lines, left y-axis) and the cumulative probability distribution (dashed lines, right y-axis) for the eccentricity of binary primordial black hole inspiral with component masses $0.01/0.1/1 M_\odot$ at gravitational-wave frequency 10 Hz.

We further investigate the impact of M_{PBH} and v_{rel} on the eccentricity distribution. In Fig. 4, the mass M_{PBH} is fixed to $0.1 M_\odot$, and the initial relative velocity v_{rel} is chosen to be 20/200/2000 m/s. The $e^{10\text{Hz}}$ results show that a higher relative velocity leads to the formation of more eccentric binaries. The cutoff for each distribution at the lowest eccentricity in Fig. 4 represents the binaries that would have been circularized the most at the gravitational wave frequency 10 Hz and are from those with

the widest separation at initial formation and thus the lowest initial eccentricity, as can be seen from Eq. (12).

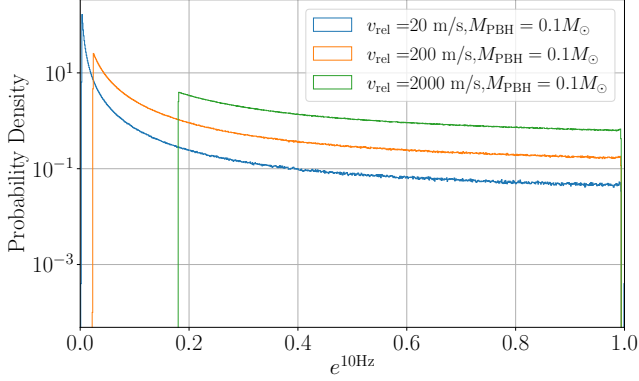


Figure 4. The eccentricity distribution at 10 Hz for primordial black hole binaries with $M_{\text{PBH}} = 0.1 M_{\odot}$ for three choices of relative velocity, 20/200/2000 m/s.

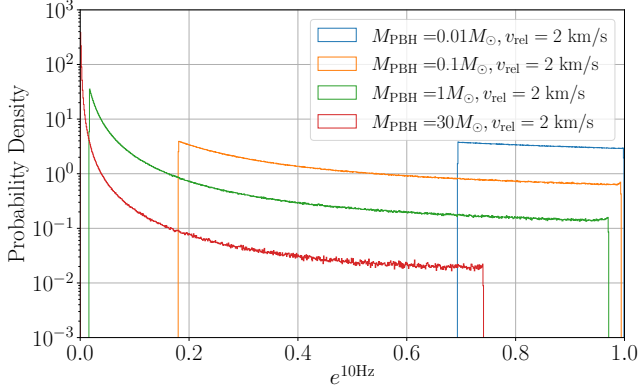


Figure 5. The eccentricity distribution at 10 Hz for primordial black hole binaries with $M_{\text{PBH}} = 0.01/0.1/1/30 M_{\odot}$ with relative velocity fixed to 2 km/s.

The eccentricity distribution for fixed v_{rel} but different masses are shown in Fig. 5. The relative velocity is chosen to be 2 km/s, which is the typical velocity for $10^6 M_{\odot}$ dark matter halos. The black hole mass is chosen to be 0.01/0.1/1/30 M_{\odot} . As considered by Cholis et al. (2016) and shown in Fig. 5, a majority of 30 M_{\odot} binary black holes have eccentricity near 0 at 10 Hz. However, the subsolar mass binaries all have nonzero peaks for eccentricity. In particular, for 0.01 M_{\odot} primordial black holes in the $10^6 M_{\odot}$ dark matter halos, all binaries have high eccentricity not lower than 0.7 at formation. Similarly, the lowest eccentricity cutoff for each distribution represents the most circularized binaries in the simulated sources.

The above numerical results show that subsolar mass compact binaries with high initial relative velocity tend

to be more eccentric compared to the more massive binary black holes with low relative velocity. Therefore, the impact of eccentricity on targeted gravitational-wave searches for subsolar mass compact binary coalescences deserves a more detailed study. We present our investigation in the next section.

3. IMPACT OF ECCENTRICITY ON GRAVITATIONAL-WAVE SEARCHES

There has been one search targeting gravitational waves from eccentric compact binary coalescence using model-based matched filtering (Nitz et al. 2020), where the authors searched for signals from eccentric binary neutron star mergers. The LIGO and Virgo Scientific Collaborations have also performed a nonmodelled generic search for eccentric binary black hole mergers (Abbott et al. 2019). Most targeted searches for compact binary coalescence use quasi-circular orbit waveform template banks, including the direct searches for subsolar mass black holes (Abbott et al. 2018a, 2019; Nitz & Wang 2021),

As demonstrated in section 2, subsolar mass primordial black holes can retain nonzero eccentricity in the LIGO and Virgo frequency band if they form in the late universe through dynamical capture. We aim to quantitatively study the potential loss in detection sensitivity when using only quasi-circular waveform template banks to search for signals from eccentric binary primordial black holes. To quantify the S/N of gravitational-wave detection, we define the following noise-weighted inner product

$$(h_1, h_2) = 4\Re \int \frac{h_1(f)h_2^*(f)}{S_n(f)} df \quad (16)$$

where h_1 and h_2 are signals or gravitational-wave templates in the Fourier domain and $S_n(f)$ is the one-sided noise power spectral density. In this section we only consider the Advanced LIGO design sensitivity in the frequency range of [20, 1024] Hz. The matched-filter S/N between the detector output s and the template h is defined to be

$$\rho = \frac{(s, h)}{\sqrt{(h, h)}}. \quad (17)$$

To measure the similarity between two waveform templates h_1 and h_2 , the overlap function is defined as the normalized inner product

$$\mathcal{O}(h_1, h_2) = \frac{(h_1, h_2)}{\sqrt{(h_1, h_1)(h_2, h_2)}}. \quad (18)$$

Two templates may be different up to a constant time and phase in the Fourier domain, thus the match function between two waveforms is given by maximizing over

the offset of coalescence time t_c and an overall phase ϕ_c

$$\mathcal{M}(h_1, h_2) = \max_{t_c, \phi_c} \left(\mathcal{O}(h_1, h_2 e^{i(2\pi f t_c - \phi_c)}) \right). \quad (19)$$

There have been several waveform approximants modeling eccentric compact binary coalescence, such as Moore et al. (2016); Huerta et al. (2018); Liu et al. (2020); Chiamello & Nagar (2020). In this work, we utilize the model proposed by Moore & Yunes (2019); Moore & Yunes (2020); Moore et al. (2018), referred to as **TaylorF2e**¹, for speedy waveform generation. **TaylorF2e** is an inspiral waveform developed in the Fourier domain and is accurate to the third post-Newtonian order. The eccentricity is valid up to at least 0.8 in the low-mass case $\sim 1 M_\odot$ (Moore & Yunes 2020), which is sufficient for our purpose to investigate the eccentricity of subsolar mass compact binaries.

In order to extract gravitational-wave signals in the data, a targeted search (Usman et al. 2016; Messick et al. 2017) builds a precalculated template bank to match filter the data. To measure the detection ability of a template bank built with quasi-circular waveforms to search for eccentric binaries, we first generate a template bank by a geometric method based on hexagonal lattice placement (Cokelaer 2007; Brown et al. 2012) using the quasi-circular waveform approximant **TaylorF2** (Buonanno et al. 2009). For this study, we assume the component black holes will have negligible spin. The template bank is designed to recover sources with component masses in the range $[0.1, 1] M_\odot$. The bank is discrete in the parameter space, and we require the maximum mismatch due to discreteness is no higher than 3% by construction. The above setting results in a bank with 6995517 templates.

Next we generate simulated gravitational-wave data with a source population using the **TaylorF2e** approximant. The mock data are then compared with every template in the bank using Eq. (19) to obtain the maximum match “fitting factor” over the entire template bank. A fitting factor of x would lead to a $1 - x^3$ loss of the detection rate for a search with a fixed amount of noise, as the gravitational-wave search S/N would be decreased to x times the theoretically optimal value.

In Fig. 6, we generate eccentric subsolar mass binary black hole gravitational-wave signals and compute the fitting factor with respect to the noneccentric template bank. Each point in the figure represents a mock signal injection.

In the left panel of Fig. 6, the binaries are chosen to have equal mass. M_{PBH} and $e^{10\text{Hz}}$ are uniformly distributed in $[0.1, 1] M_\odot$ and $[0, 0.2]$, respectively. The fitting factor for $e^{10\text{Hz}}$ and the chirp mass $M_{\text{chirp}} = (m_1 m_2)^{3/5} (m_1 + m_2)^{1/5}$ ($\sim 0.87 M_{\text{PBH}}$ for equal mass) is presented. The figure also illustrates the 97% and 80% contour lines obtained from fitting the plot. The figure shows the trend that the fitting factor gets worse for higher eccentricity, and also for lighter binaries because of their longer duration. For a component mass $m = 0.1/1 M_\odot$, the fitting factor drops below 97% with $e^{10\text{Hz}} \geq 0.003/0.20$.

In the right panel of Fig. 6, we consider the impact on fitting factor from different mass ratios by fixing $M_{\text{chirp}} = 0.4 M_\odot$. The mass ratio is uniformly distributed in $[1, 4]$ and the eccentricity is uniformly in $[0, 0.2]$. As shown, the 97% and 80% fitting factor lines only depend weakly on the mass ratio and decrease for higher mass ratio.

We also consider more realistic distributions for $e^{10\text{Hz}}$ as derived in Fig. 3 of Section 2. We generate two groups of mock data each with ~ 2000 signals using **TaylorF2e**. The component mass is $0.1 M_\odot$ and $1 M_\odot$, respectively, and only equal-mass binaries are considered. The inclination angle is chosen to be uniformly distributed in $[-\pi/2, \pi/2]$, the polarization angle is uniformly in $[0, 2\pi]$, and the source sky location is isotropic. The eccentricity distribution is drawn from Fig. 3 for $0.1 M_\odot$ and $1 M_\odot$ sources accordingly.

The cumulative probability with respect to the fitting factor is shown in Fig. 7. The vertical dashed line in Fig. 7 denotes 97%, which all the signals with zero eccentricity should exceed by construction of the template bank. However, due to the existence of eccentricity, for $M_{\text{PBH}} = 0.1 M_\odot$, up to 68% of the signals have a fitting factor lower than 97%, and 41% have a fitting factor lower than 80%. For $M_{\text{PBH}} = 1 M_\odot$, 15% of the signals have a fitting factor lower than 97%, and 6% of the signals have a fitting factor lower than 80%. Also note that, when the fitting factor is low, the mismatch between signals and templates may be significant enough to cause issues with signal-based vetoes (Allen 2005) which would further reduce the detection rate of eccentric sources. Therefore our results based on the fitting factor are a conservative estimation for the loss of detection rate.

Given that the fitting factor can only measure the fractional recovered S/N for a single injected signal, we use the effective fitting factor FF_{eff} (Harry et al. 2016, 2014; Buonanno et al. 2003) to account for the overall fraction for detection loss for a whole group of simulated signals. The effective fitting factor is defined as a mean average

¹ The source code can be found in <https://github.com/gwastro/TaylorF2e>

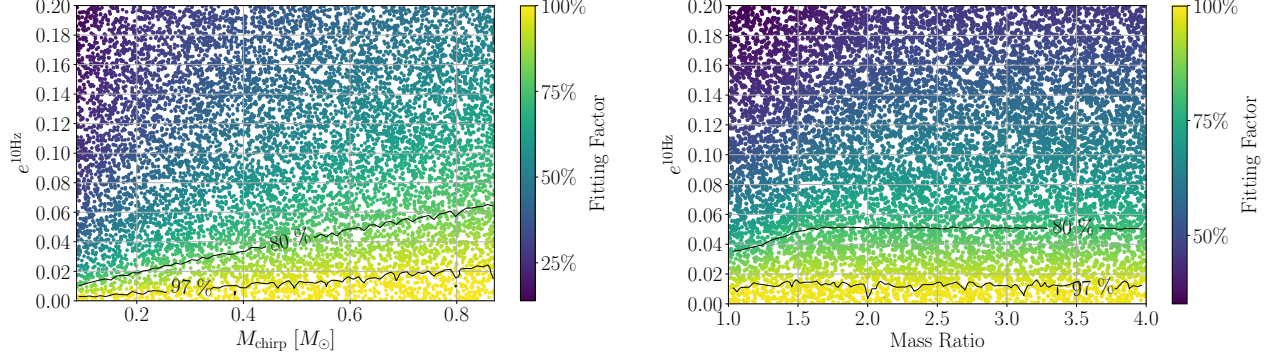


Figure 6. The fitting factor for simulated data of eccentric subsolar binary black hole coalescences with respect to the template bank constructed from a quasi-circular waveform approximant. Each point represents an injected mock signal. In the left panel, the signals are generated from equal-mass binaries with a component mass in $[0.1, 1] M_\odot$ uniformly. In the right panel, the chirp mass is fixed to $0.4 M_\odot$ and the mass ratio is in $[1, 4]$.

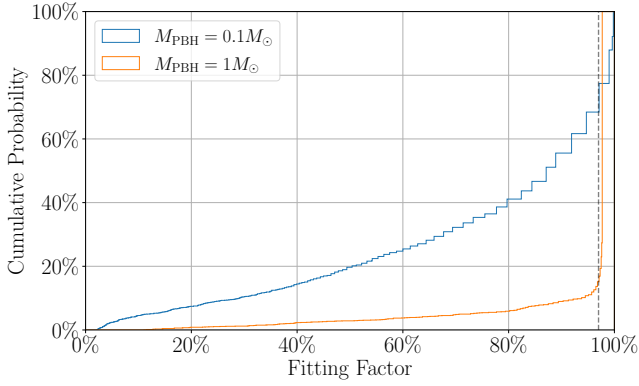


Figure 7. Cumulative distribution for the fitting factor for gravitational-wave sources with $0.1 M_\odot$ and $1 M_\odot$ and eccentricity distributions derived from Section 2. The vertical dashed line denotes 97%, which represents the lower limit for the fitting factor for signals without eccentricity.

of fitting factors weighted by the signal amplitude

$$FF_{\text{eff}} = \left(\frac{\sum_{i=1}^N FF_i^3 \sigma_i^3}{\sum_{i=1}^N \sigma_i^3} \right)^{1/3}, \quad (20)$$

where the subscript i denotes the i -th mock injection, N is the total number of signals, FF_i is the fitting factor, and $\sigma_i = \sqrt{(h_i|h_i)}$ is the optimal S/N for the i -th signal. An effective fitting factor of x would lead to a $1 - x^3$ loss of detection rate.

For our two groups of injection with $M_{\text{PBH}} = 0.1 M_\odot$ and $1 M_\odot$, $FF_{\text{eff}} = 83\%$ and 95.8% , respectively, which corresponds to an overall loss of 42% and 12% of signals compared to the idealized maximum. For comparison, if only selecting the injected signals with $e^{10\text{Hz}} = 0$, the effective fitting factor is 99.7% for $M_{\text{PBH}} = 0.1 M_\odot$ and 97.8% for $M_{\text{PBH}} = 1 M_\odot$, which corresponds to a 0.9% and 6.4% loss, which arises from the discreteness of template bank. After subtracting the signals missed due to

template bank discreteness, for $M_{\text{PBH}} = 0.1 M_\odot$ and $M_{\text{PBH}} = 1 M_\odot$ sources within the late-universe dynamical encounter model, we conclude that the eccentricity effects can lead to loss of 41% and 6% of the signals, respectively, by a targeted search with a quasi-circular waveform template bank using Advanced LIGO at its designed sensitivity. For primordial black holes with an extended mass in the range $[0.1, 1] M_\odot$, we expect the the corresponding results for loss of detection should lie in between these.

4. DISCUSSIONS AND CONCLUSIONS

In this work, we investigate the prospects for detecting gravitational-wave signals from eccentric subsolar mass binary black hole inspirals, which would be a signature for primordial black hole binaries formed by dynamical capture in the local universe. The merger rate and eccentricity distribution for binaries assuming a delta function mass distribution varying in $[0.01, 1] M_\odot$ are derived. For $1 M_\odot - 1 M_\odot$ binaries, the detection rate is $\mathcal{O}(1)/\text{yr}$ for Advanced LIGO and Virgo with design sensitivity, if primordial black holes account for a majority of dark matter, and 12%(3%) of the sources have $e^{10\text{Hz}} \geq 0.01(0.1)$, thus eccentric signals may be detected with a few years of observation based on the assumed model. For $0.1 - 0.1 M_\odot$ and $0.01 - 0.01 M_\odot$ binaries the detection rate would be too low for the second generation ground-based detectors, but it is promising for detection by the third generation detectors. Conversely, nondetection in the future would put constraints on our understanding of this formation channel.

We also investigate what fraction of the eccentric binaries can be missed by using quasi-circular waveform template bank. Results show that current targeted searches can miss 41% and 6% of the events with component masses of $0.1 M_\odot$ and $1 M_\odot$, respectively, with Advanced

LIGO designed sensitivity, due to the eccentricity of primordial black hole binaries arising from dynamical encounter in the local universe.

For the formation scenario of primordial black hole binaries, we only consider the two-body direct capture through gravitational-wave braking. Other mechanisms such as three-body interaction via Kozai-Lidov effects (Kozai 1962; Lidov 1962) may further improve the event rate, and would be interesting to consider in a future work.

Third generation gravitational-wave detectors such as Cosmic Explorer (Reitze et al. 2019) and Einstein Telescope (Punturo et al. 2010) are being planned. The detection volume is expected to increase by three orders of magnitude compared to the second generation. Moreover, the sensitive band can be pushed down to ~ 2 Hz,

at which the eccentricity for primordial black hole binaries is more significant than later at 10 Hz as considered in this work. Third generation detectors are even more promising for hunting for eccentric gravitational-waves signals.

The code and data associated with this work are available at <https://github.com/gwastro/prospects-subsolarmass-ecc>.

ACKNOWLEDGMENTS

We acknowledge the Max Planck Gesellschaft for support and the Atlas cluster computing team at AEI Hannover.

REFERENCES

- Aasi, J., et al. 2015, *Class. Quantum Grav.*, 32, 074001, doi: [10.1088/0264-9381/32/7/074001](https://doi.org/10.1088/0264-9381/32/7/074001)
- Abbott, B., et al. 2019, *Astrophys. J.*, 883, 149, doi: [10.3847/1538-4357/ab3c2d](https://doi.org/10.3847/1538-4357/ab3c2d)
- Abbott, B. P., Abbott, R., Abbott, T. D., et al. 2016a, *ApJL*, 833, L1, doi: [10.3847/2041-8205/833/1/L1](https://doi.org/10.3847/2041-8205/833/1/L1)
- . 2016b, *ApJS*, 227, 14, doi: [10.3847/0067-0049/227/2/14](https://doi.org/10.3847/0067-0049/227/2/14)
- . 2017, *Nature*, 551, 85, doi: [10.1038/nature24471](https://doi.org/10.1038/nature24471)
- . 2018a, *PhRvL*, 121, 231103, doi: [10.1103/PhysRevLett.121.231103](https://doi.org/10.1103/PhysRevLett.121.231103)
- . 2018b, *Living Reviews in Relativity*, 21, 3, doi: [10.1007/s41114-018-0012-9](https://doi.org/10.1007/s41114-018-0012-9)
- . 2019, *PhRvD*, 100, 024017, doi: [10.1103/PhysRevD.100.024017](https://doi.org/10.1103/PhysRevD.100.024017)
- Abbott, R., Abbott, T. D., Abraham, S., et al. 2020, *arXiv e-prints*, arXiv:2010.14527, <https://arxiv.org/abs/2010.14527>
- Acernese, F., et al. 2015, *Class. Quantum Grav.*, 32, 024001, doi: [10.1088/0264-9381/32/2/024001](https://doi.org/10.1088/0264-9381/32/2/024001)
- Ali-Haïmoud, Y., Kovetz, E. D., & Kamionkowski, M. 2017, *PhRvD*, 96, 123523, doi: [10.1103/PhysRevD.96.123523](https://doi.org/10.1103/PhysRevD.96.123523)
- Allen, B. 2005, *Phys. Rev. D*, 71, 062001, doi: [10.1103/PhysRevD.71.062001](https://doi.org/10.1103/PhysRevD.71.062001)
- Bird, S., Cholis, I., Muñoz, J. B., et al. 2016, *PhRvL*, 116, 201301, doi: [10.1103/PhysRevLett.116.201301](https://doi.org/10.1103/PhysRevLett.116.201301)
- Boehm, C., Kobakhidze, A., O’hare, C. A. J., Picker, Z. S. C., & Sakellariadou, M. 2021, *JCAP*, 03, 078, doi: [10.1088/1475-7516/2021/03/078](https://doi.org/10.1088/1475-7516/2021/03/078)
- Brown, D. A., Harry, I., Lundgren, A., & Nitz, A. H. 2012, *Phys. Rev. D*, 86, 084017, doi: [10.1103/PhysRevD.86.084017](https://doi.org/10.1103/PhysRevD.86.084017)
- Buonanno, A., Chen, Y.-b., & Vallisneri, M. 2003, *Phys. Rev. D*, 67, 104025, doi: [10.1103/PhysRevD.67.104025](https://doi.org/10.1103/PhysRevD.67.104025)
- Buonanno, A., Iyer, B. R., Ochsner, E., Pan, Y., & Sathyaprakash, B. S. 2009, *PhRvD*, 80, 084043, doi: [10.1103/PhysRevD.80.084043](https://doi.org/10.1103/PhysRevD.80.084043)
- Byrnes, C. T., Hindmarsh, M., Young, S., & Hawkins, M. R. S. 2018, *JCAP*, 08, 041, doi: [10.1088/1475-7516/2018/08/041](https://doi.org/10.1088/1475-7516/2018/08/041)
- Carr, B., Clesse, S., García-Bellido, J., & Kühnel, F. 2021, *Phys. Dark Univ.*, 31, 100755, doi: [10.1016/j.dark.2020.100755](https://doi.org/10.1016/j.dark.2020.100755)
- Carr, B., & Kühnel, F. 2020, *Ann. Rev. Nucl. Part. Sci.*, 70, 355, doi: [10.1146/annurev-nucl-050520-125911](https://doi.org/10.1146/annurev-nucl-050520-125911)
- Carr, B. J., & Hawking, S. W. 1974, *MNRAS*, 168, 399, doi: [10.1093/mnras/168.2.399](https://doi.org/10.1093/mnras/168.2.399)
- Chiaromello, D., & Nagar, A. 2020, *PhRvD*, 101, 101501, doi: [10.1103/PhysRevD.101.101501](https://doi.org/10.1103/PhysRevD.101.101501)
- Cholis, I., Kovetz, E. D., Ali-Haïmoud, Y., et al. 2016, *PhRvD*, 94, 084013, doi: [10.1103/PhysRevD.94.084013](https://doi.org/10.1103/PhysRevD.94.084013)
- Cokelaer, T. 2007, *PhRvD*, 76, 102004, doi: [10.1103/PhysRevD.76.102004](https://doi.org/10.1103/PhysRevD.76.102004)
- Diemer, B. 2018, *ApJS*, 239, 35, doi: [10.3847/1538-4365/aee8c](https://doi.org/10.3847/1538-4365/aee8c)
- Dutton, A. A., & Macciò, A. V. 2014, *MNRAS*, 441, 3359, doi: [10.1093/mnras/stu742](https://doi.org/10.1093/mnras/stu742)
- Green, A. M., & Kavanagh, B. J. 2021, *J. Phys. G*, 48, 4, doi: [10.1088/1361-6471/abc534](https://doi.org/10.1088/1361-6471/abc534)
- Harry, I., Privitera, S., Bohé, A., & Buonanno, A. 2016, *PhRvD*, 94, 024012, doi: [10.1103/PhysRevD.94.024012](https://doi.org/10.1103/PhysRevD.94.024012)
- Harry, I. W., Nitz, A. H., Brown, D. A., et al. 2014, *PhRvD*, 89, 024010, doi: [10.1103/PhysRevD.89.024010](https://doi.org/10.1103/PhysRevD.89.024010)

- Hawking, S. 1971, MNRAS, 152, 75,
doi: [10.1093/mnras/152.1.75](https://doi.org/10.1093/mnras/152.1.75)
- Huerta, E. A., Moore, C. J., Kumar, P., et al. 2018, PhRvD, 97, 024031, doi: [10.1103/PhysRevD.97.024031](https://doi.org/10.1103/PhysRevD.97.024031)
- Jedamzik, K. 1997, Phys. Rev. D, 55, 5871,
doi: [10.1103/PhysRevD.55.R5871](https://doi.org/10.1103/PhysRevD.55.R5871)
- . 2021, Phys. Rev. Lett., 126, 051302,
doi: [10.1103/PhysRevLett.126.051302](https://doi.org/10.1103/PhysRevLett.126.051302)
- Kozai, Y. 1962, AJ, 67, 591, doi: [10.1086/108790](https://doi.org/10.1086/108790)
- Lidov, M. L. 1962, Planet. Space Sci., 9, 719,
doi: [10.1016/0032-0633\(62\)90129-0](https://doi.org/10.1016/0032-0633(62)90129-0)
- Liu, X., Cao, Z., & Shao, L. 2020, PhRvD, 101, 044049,
doi: [10.1103/PhysRevD.101.044049](https://doi.org/10.1103/PhysRevD.101.044049)
- Maggiore, M. 2008, Gravitational Waves: Volume 1: Theory and Experiments, Gravitational Waves (OUP Oxford).
<https://books.google.de/books?id=AqVpQgAACAAJ>
- Messick, C., Blackburn, K., Brady, P., et al. 2017, PhRvD, 95, 042001, doi: [10.1103/PhysRevD.95.042001](https://doi.org/10.1103/PhysRevD.95.042001)
- Moore, B., Favata, M., Arun, K. G., & Mishra, C. K. 2016, PhRvD, 93, 124061, doi: [10.1103/PhysRevD.93.124061](https://doi.org/10.1103/PhysRevD.93.124061)
- Moore, B., Robson, T., Loutrel, N., & Yunes, N. 2018, Classical and Quantum Gravity, 35, 235006,
doi: [10.1088/1361-6382/aaea00](https://doi.org/10.1088/1361-6382/aaea00)
- Moore, B., & Yunes, N. 2019, Classical and Quantum Gravity, 36, 185003, doi: [10.1088/1361-6382/ab3778](https://doi.org/10.1088/1361-6382/ab3778)
- Moore, B., & Yunes, N. 2020, Class. Quant. Grav., 37, 225015, doi: [10.1088/1361-6382/ab7963](https://doi.org/10.1088/1361-6382/ab7963)
- Nakamura, T., Sasaki, M., Tanaka, T., & Thorne, K. S. 1997, ApJL, 487, L139, doi: [10.1086/310886](https://doi.org/10.1086/310886)
- Navarro, J. F., Frenk, C. S., & White, S. D. M. 1996, ApJ, 462, 563, doi: [10.1086/177173](https://doi.org/10.1086/177173)
- Nitz, A. H., Lenon, A., & Brown, D. A. 2020, ApJ, 890, 1,
doi: [10.3847/1538-4357/ab6611](https://doi.org/10.3847/1538-4357/ab6611)
- Nitz, A. H., & Wang, Y.-F. 2021, Phys. Rev. Lett., 126, 021103, doi: [10.1103/PhysRevLett.126.021103](https://doi.org/10.1103/PhysRevLett.126.021103)
- Nitz, A. H., Dent, T., Davies, G. S., et al. 2019, Astrophys. J., 891, 123, doi: [10.3847/1538-4357/ab733f](https://doi.org/10.3847/1538-4357/ab733f)
- O’Leary, R. M., Kocsis, B., & Loeb, A. 2009, MNRAS, 395, 2127, doi: [10.1111/j.1365-2966.2009.14653.x](https://doi.org/10.1111/j.1365-2966.2009.14653.x)
- Peters, P. C. 1964, Physical Review, 136, 1224,
doi: [10.1103/PhysRev.136.B1224](https://doi.org/10.1103/PhysRev.136.B1224)
- Peters, P. C., & Mathews, J. 1963, Physical Review, 131, 435, doi: [10.1103/PhysRev.131.435](https://doi.org/10.1103/PhysRev.131.435)
- Prada, F., Klypin, A. A., Cuesta, A. J., Betancort-Rijo, J. E., & Primack, J. 2012, MNRAS, 423, 3018,
doi: [10.1111/j.1365-2966.2012.21007.x](https://doi.org/10.1111/j.1365-2966.2012.21007.x)
- Punturo, M., Abernathy, M., Acernese, F., et al. 2010, Classical and Quantum Gravity, 27, 194002,
doi: [10.1088/0264-9381/27/19/194002](https://doi.org/10.1088/0264-9381/27/19/194002)
- Raeymaekers, J. 2007, Fortschritte der Physik, 55, 811,
doi: [10.1002/prop.200610362](https://doi.org/10.1002/prop.200610362)
- Raidal, M., Spethmann, C., Vaskonen, V., & Veermäe, H. 2019, JCAP, 02, 018,
doi: [10.1088/1475-7516/2019/02/018](https://doi.org/10.1088/1475-7516/2019/02/018)
- Reitze, D., Adhikari, R. X., Ballmer, S., et al. 2019, in Bulletin of the American Astronomical Society, Vol. 51, 35. <https://arxiv.org/abs/1907.04833>
- Sasaki, M., Suyama, T., Tanaka, T., & Yokoyama, S. 2016, PhRvL, 117, 061101,
doi: [10.1103/PhysRevLett.117.061101](https://doi.org/10.1103/PhysRevLett.117.061101)
- Suwa, Y., Yoshida, T., Shibata, M., Umeda, H., & Takahashi, K. 2018, MNRAS, 481, 3305,
doi: [10.1093/mnras/sty2460](https://doi.org/10.1093/mnras/sty2460)
- The LIGO Scientific Collaboration, the Virgo Collaboration, Abbott, R., et al. 2020a, arXiv e-prints, arXiv:2010.14533. <https://arxiv.org/abs/2010.14533>
- . 2020b, arXiv e-prints, arXiv:2010.14529. <https://arxiv.org/abs/2010.14529>
- Timmes, F. X., Woosley, S. E., & Weaver, T. A. 1996, ApJ, 457, 834, doi: [10.1086/176778](https://doi.org/10.1086/176778)
- Tinker, J., Kravtsov, A. V., Klypin, A., et al. 2008, ApJ, 688, 709, doi: [10.1086/591439](https://doi.org/10.1086/591439)
- Turner, M. 1977, ApJ, 216, 610, doi: [10.1086/155501](https://doi.org/10.1086/155501)
- Usman, S. A., Nitz, A. H., Harry, I. W., et al. 2016, Classical and Quantum Gravity, 33, 215004,
doi: [10.1088/0264-9381/33/21/215004](https://doi.org/10.1088/0264-9381/33/21/215004)
- Vaskonen, V., & Veermäe, H. 2020, Phys. Rev. D, 101, 043015, doi: [10.1103/PhysRevD.101.043015](https://doi.org/10.1103/PhysRevD.101.043015)
- Zel’dovich, Y. B., & Novikov, I. D. 1967, Soviet Ast., 10, 602